Supporting Information

Ulusoy et al. 10.1073/pnas.1003432107

SI Methods

Experimental Design. A total of 117 young adult female Sprague-Dawley rats weighing between 225–250 g were obtained from Charles River. The animals were housed under a 12-h light/12-h dark cycle with free access to food and water. All surgical procedures were performed according to the regulations set by the ethical committee for use of laboratory animals in Lund-Malmö region.

The animals were divided into four experimental groups. Two group of animals were injected with rAAV5 vectors expressing either the TH knockdown construct (shTH group; $n = 32$) or its scrambled control (shTHscr group; $n = 27$), a third group that received striatal 6-hydroxydopamine lesion (6-OHDA group; $n = 26$) and finally a forth group of rats ($n = 23$) were followed as nontreated intact animals. All animals were allowed to survive for 5 mo before any other treatment was initiated. At that time point, animals in each group were divided into 6 subsets. The first subset consisting of 14 animals (shTH $n = 4$, shTHscr $n = 4$, 6-OHDA $n = 3$, intact $n = 3$) was directly killed and the brains were fixed for histological analysis. The second subset, consisting of 14 animals (shTH $n = 3$, shTHscr $n = 3$, 6-OHDA $n = 4$, intact $n = 4$) was included in the microdialysis experiment and then killed for histological analysis. Two additional subsets consisting of a total of 37 animals (shTH $n = 6 + 6$, shTHscr $n = 5 + 4$, 6-OHDA $n = 4 + 3$, intact $n = 4 + 5$) were included in biochemical analysis either at baseline or after a single dose L-DOPA challenge. Two final subsets consisting of a total of 43 animals were allocated into behavioral test paradigms with chronic L-DOPA (presynaptic induction of dyskinesias) or Apomorphine (postsynaptic induction of dyskinesias) treatment regimens (shTH $n = 8 + 5$, shTHscr $n = 6 + 5$, 6-OHDA $n = 7 + 5$, intact $n = 4 + 3$, respectively) and then killed for histological analysis.

Constructs and rAAV5 Virus Production. The rAAV5 vectors expressing short hairpin RNA (shRNA) sequences were generated as previously described (1). Briefly, an siRNA matching the rat TH mRNA at 790–810bp location and the corresponding scrambled siRNA sequence (denoted as shTH and shTHscr, respectively) were inserted into the transfer plasmid for vector production. The sequences for these shRNAs were as follows: shTH (5′-aacggtactgtggctaccgagttcaagagactcggtagccacagtaccgtt-3′) and shTHscr (5′-gcgcgtcagtcaggtacagatttcaagagaatctgtacctgactgacgcgc-3′). These sequences were cloned into an AAV transfer vector in two steps. First, the shRNA sequences were placed downstream of the H1 promoter. In the second step, XhoI-SacI fragments containing the H1-shRNA sequences were cloned into the pTR-UF11 backbone plasmid containing the AAV2 inverted terminal repeats. The insertion was carried out by removing PYF441 enhancer and HSV-tk promoter driven *NeoR* gene on the original backbone plasmid (pTR-UF11), which was downstream of GFP driven by a CMV enhancer hybrid CBA promoter. rAAV5 vectors were produced in 293 cells in cell factories with a confluency of 70–80%. The transfection was carried out using the Calcium-phosphate method and included the appropriate transfer plasmid (as detailed above) and the pXYZ5 packaging plasmid, encoding for the AAV5 capsid proteins in trans (2, 3). Transfected cells were incubated for 3 d before being harvested by PBS-EDTA. The cell pellet was lysed and crude lysates were purified first by ultracentrifugation (1.5 h at 350,000 × *g* at 18 °C) in a discontinuous iodixanol gradient, and then by ion-exchange chromatography using FPLC as described earlier (1). The virus suspension was then concentrated using a concentrator (Ultra 100kDa MWCO; Millipore Amicon) at 1,500 × *g* and 18 °C in two consecutive steps by adding lactated ringer. The titers of the vector preparations were determined using TaqMan quantitative PCR. The stock batch titers were 3.7E12 and 3.6E13 gc/mL for shTH and shTHscr, respectively. The injected solution was adjusted to the target concentration [as determined in (1)] by a dilution from the stocks in PBS buffer. The final injected solution was retitered before use and confirmed to have 1.3E12 and 1.7E12 gc/mL for the vector encoding for shTH and shTHscr, respectively.

Stereotaxic Surgeries. Viral vector injection and 6-OHDA lesion surgeries were performed under 20:1 mixture of fentanylcitrate (Fentanyl) and medetomidin hydrochloride (Dormitor) (Apoteksbolaget) prepared as an injectable anesthesic. rAAV5 vector injections were made into substantia nigra using 5-μL Hamilton syringe fitted with a glass capillary with a tip diameter of about 60–80 μm. Two microliters of the buffer containing the appropriate number of viral particles was injected at a speed of 0.4 μL/min. The needle was withdrawn slowly 5 min after completion of the injection. Coordinates used for SN injections were anteroposterior (AP): −5.2 mm and mediolateral (ML): −2.0 mm relative to the bregma and dorsoventral (DV): −7.2 mm from the dural surface, according to the atlas of Paxinos and Watson (4). The tooth bar was adjusted to −2.3 mm in all nigral injections. 6-OHDA lesions were placed into the right striatum by injecting a total of 21 μg 6-OHDA dissolved in ascorbate-saline (0.02%) delivered in three deposits distributed along the rostrocaudal axis. The coordinates were AP: +1.0, −0.1, −1.2 mm and ML: −3.0, −3.7, −4.5 mm, respectively, relative to the bregma and DV: −5.0 mm from the dural surface (5). The tooth bar was set to 0.0 mm. A volume of 2 μL per site was injected at a rate of 0.4 μL/min. The needle was left in place for 5 min after completion of each injection.

Microdialysis Experiment. The in vivo DOPA synthesis and DA release parameters in the striatum were assessed using a microdialysis protocol. For this purpose, the rats were anesthesized with 1–2% isofluorane mixed with O_2 and N_2O and placed in a stereotaxic frame. Microdialysis probes used in this experiment had a 3-mm membrane length and 0.5-mm outer diameter (Agnthos Microdialysis). The probes were inserted into the striatum with the help of a holder and placed at AP: +0.6 mm, ML: −3.0 mm relative to bregma and DV: −5.5 mm from the dural surface. The tooth bar was set to −2.3 mm.

The probes were connected to a syringe infusion pump (Model 100; CMA Microdialysis) via polyethylene tubing and perfused with normal ringer solution containing 145 mM NaCl, 3 mM KCl and 1.3 mM $CaCl_2$ at a constant rate of 1 μL/min. The dialysates were directly analyzed on Alexys online monoamine analyzer microdialysis system (Antec Leyden) consisting of a DECADE II electrochemical detector and VT-3 electrochemical flow cell. The outlet of the microdialysis probe was connected to a 14-port external valve that can direct the dialysate into two separate flow paths (Fig. S2). Two different mobile phases—optimized for the detection of the respective metabolites—were used in each of the two flow paths. The first mobile phase (50 mM phosphoric acid, 8 mM NaCl, 0.1 mM EDTA, 12.5% methanol, 500 mg/L octane sulfate; pH 6.0) was used for the detection of DA and 5-HT ran through a 1 mm × 50-mm column with 3 μm particle size (ALF-105) at a flow rate of 75 μL/min. The second mobile phase (50 mM phosphoric acid, 50 mM citric acid, 8 mM NaCl, 0.1 mM EDTA, 10% methanol, 600 mg/L octane sulfate; pH 3.2) was used for the detection of DOPA, DOPAC, HVA, and 5-HIAA, which passed through a 1 mm × 150-mm column with 3-μm particle size (ALF-115) at a flow rate of 100 μL/min. The dialysate samples were

transferred via 5-μL loops simultaneously into each flow path and analyzed by the online HPLC at 12.5 min time bins.

One hour of equilibration was followed by analysis of three baseline samples before the dialysate was changed to a modified ringer lactate solution containing high KCl (51 mM NaCl, 100 mM KCl, and 1.3 mM $CaCl_2$) for 12.5 min to stimulate the readily releasable pool of DA and then switched back to the normal ringer lactate solution. After analyzing serial samples for six more time bins (i.e., until t = 125 min), the animals were i.p. injected with 100 mg/kg of NSD-1015 (Sigma-Aldrich) to block the AADC enzyme activity. The dialysate samples were analyzed for another 75 min following the NSD-1015 treatment while the newly synthesized DOPA accumulated in the brain. The chromatograms were analyzed using the Clarity Chromatographic Station (version 2.7.03.498; DataApex). The probes were withdrawn at the end of the procedure and animals were allowed to recover and kept alive for another 10 d before killing.

Apomorphine and L-DOPA–Induced AIMs. The animals included in the behavioral experiments were treated as follows: L-DOPA treatment regimen was carried as consecutive weekly escalating doses of 6, 12, and 24 mg/kg daily L-DOPA administered s.c. together with 10 mg/kg benserazide over a 3-wk period. AIMs were evaluated three times (the first, third or forth, and the final day) at each dose level. On the 22nd day of the treatment the animals were injected with a final dose of 24 mg/kg L-DOPA 2 h before death. The apomorphine treatment regimen was carried out as three consecutive 5-d escalating doses of 0.1, 0.2, and 0.5 mg/kg daily apomorphine injections (dissolved in 0.2 mg/mL ascorbate-saline and administered s.c.) over a 15-d treatment period. A group of animals from the 6-OHDA group (n = 4) and intact group (n = 3) were used as sham controls and received s.c. injection of 0.2 mg/mL ascorbate-saline for 3 wk. The evolution of AIMs was monitored on alternating days during the treatment period (i.e., on first, third, and last days of each dose). On day 16, a subset of the animals received a single challenge dose of 24 mg/kg L-DOPA, to test the ability to trigger AIMs via the presynaptic mechanism in apomorphine primed animals and killed 2 h after the drug administration.

The evaluation of the AIMs were performed according to the rat dyskinesia scale as described previously (6, 7). Briefly, the animals were placed individually in transparent plastic cages with a grid lid so that every movement can be visualized in detail. A researcher blinded to the identity of the animals scored them every 10 or 20 min following apomorphine or L-DOPA injections, respectively. The AIMs were classified into three subtypes according to their topographic distribution as forelimb, orolingual, and axial dyskinesias. Locomotive dyskinesia displayed as contralateral rotations were scored separately. The severity of each AIM subtype was scored from 0 to 4 (0, no abnormal behaviors detected; 1, occasional AIMs, i.e., present less than 50% of the time; 2, frequent AIMs, i.e., present more than 50% of the time; 3, continuous AIMs, but interrupted by strong sensory stimuli; and 4, continuous AIMs, not interrupted by strong sensory stimuli). Half-points were used where the behavior of the animal were clearly in between the two defined points. The data are calculated as time-integrated scores and represented by sum of the orolingual, limb and axial subtypes.

Biochemical Assays. A total of 37 animals were killed for HPLC analysis to assess the total tissue levels of DA, serotonin (5-HT), and their metabolites either at baseline (n = 19) or 150 min after a single 12 mg/kg L-DOPA injection (n = 18). For this purpose, the animals were decapitated and the brains were rapidly dissected. After a brief rinse with an ice-cold saline solution, the brains were placed on a brain slicer. A 2-mm slice containing the head of striatum and nucleus accumbens was dissected out from the surrounding tissue. This sample was then quickly dissected into two parts; one containing the ventromedial striatum together with nucleus accumbens and the other containing the rest of the dorsal striatal tissue within that segment. The tissue was rapidly frozen on dry ice and kept at −80 °C until further processing. The midbrain samples from those animals were fixed in 4% paraformaldehyde overnight for immunohistochemical detection of viral transduction and treated in the same way as described under the histological analysis section below.

At the time of analysis striatal tissue samples were sonicated in 18 mL/mg ice-cold homogenization buffer (20 mM Tris acetate, pH 6.1) and centrifuged at 20,000 × g for 10 min at 4 °C. The supernatant was filtered through a PVDF filter (0.45μm; Unifilter) and used for HPLC analysis for determination of the total tissue concentration of DA, 5-HT, and their metabolites. Briefly, 20 μL of each sample was injected by a cooled Spark Midas autosampler (Spark Holland) into an ESA Coulochem III coupled to an electrochemical detector set to a potential of +350 mV. The mobile phase (5 g/L Na acetate, 30 mg/L Na_2-EDTA, sodium octane sulphonic acid 100mg/L, 10% methanol, pH 4.2) was delivered at a flow rate of 0.5 mL/min to a reversed phase C18 column (particle size 3 μm, 4.0 mm × 100 mm, Chromtech). The peaks were analyzed by using the Clarity Chromatographic Station (DataApex). The amounts were expressed as nmol/mg tissue.

Histological Analysis. Rats were deeply anesthetized with 1.2 mL sodium pentobarbital (Apoteksbolaget). They were perfused through the ascending aorta first with 50 mL physiological saline at room temperature over 1 min and then by 250 mL ice-cold 4% paraformaldehyde (PFA) for 5 min. Brains were postfixed in 4% PFA solution for 2 h before being transferred into 25% sucrose solution for cyroprotection, where they were kept until they had sunk (typically within 24–48hrs). The brains were then sectioned in the coronal plane on a freezing microtome at a thickness of 35 μm. Sections were collected in six series and stored at −20 °C in a phosphate buffer containing 30% glycerol and 30% ethylene glycol until further processing.

Immunohistochemical stainings were performed on free-floating sections. For this purpose, brain sections were first rinsed with potassium-PBS (KPBS), and then endogenous peroxidase activity was quenched by incubation in a mixture of 3% H_2O_2 and 10% methanol in KPBS for 30 min. After three rinsing steps in KPBS, nonspecific binding sites were blocked by incubation in KPBS containing 5% normal serum matched to the species used to raise the corresponding secondary antibody and 0.25% Triton-X. Samples were then incubated overnight at room temperature in primary antibody solution containing 5% serum and 0.25% Triton-X. The primary antibodies used for immunohistochemical staining were as follows: mouse anti-TH (working dilution 1:2,000, MAB318; Millipore), rabbit anti-VMAT2 (working dilution 1:1,000, AB1767; Millipore), chicken anti-GFP (working dilution 1:5,000, ab13970; Abcam), goat anti-FosB (working dilution 1:1,000, SC-48X; Santa Cruz) and rabbit anti-c-Fos (working dilution 1:1,000, PC05; Oncogene). On the second day, the sections were rinsed in KPBS and then incubated for 1h at room temperature in 1:200 dilution of appropriate biotinylated secondary antibody solutions (horse anti-mouse for TH antibody, goat anti-rabbit for c-Fos and VMAT2 antibodies, sheep anti-goat for FosB antibody; Vector Laboratories). After rinsing, the sections were treated with avidin-biotin-peroxidase complex (ABC Elite kit; Vector Laboratories) and the color reaction was developed by incubation in 25 mg/mL 3,3′-diaminobenzidine and 0.005% H_2O_2. To increase the contrast in the FosB and c-Fos staining 2.5 mg/mL Nickel sulfate was added in the DAB solution before the color reaction. Sections were mounted on chrome-alum coated glass slides, dehydrated and cover-slipped with Depex mounting media (Sigma).

TH, GFP, and VMAT2 triple immunohistofluorescence was carried out as above with the exception that the biotinylated secondary antibodies were replaced with fluorophore conjugated

variants (Dylight 488 conjugated donkey-anti-chicken, cy3 conjugated donkey-anti-mouse conjugated, and cy5 conjugated donkey-anti-rabbit; Jackson Immunoresearch) and H_2O_2 quenching, ABC and DAB reaction steps were excluded. The sections were directly mounted on chrome-alum coated glass slides and cover-slipped using PVA-DABCO (Sigma).

Image Analysis. The optical intensity of the TH- and VMAT2-positive fibers as well as the numbers of c-Fos and FosB positive cells of the striatum were analyzed on images captured using a 10× Plan-Fluor objective (Numerical aperture = 0.30) on a Nikon Eclipse 90i microscope equipped with a Nikon DS-Q1Mc camera using NIS software (NIS Elements AR 3.0; Nikon). The fiber density measurements were performed at four rostrocaudal levels through the striatum (*i*) anterioposterior (AP), +2.16; (*ii*) AP, +0.84; (*iii*) AP, −0.3; (*iv*) AP, −0.9 relative to bregma. For the c-Fos and FosB positive cells the images were captured from three rostrocaudal striatal levels (*i*) AP, +1.20; (*ii*) AP, −0.26; and (*iii*) AP, −1.30; relative to bregma (Fig S4) according to the rat brain atlas of Paxinos and Watson (4). To estimate the specific TH and VMAT2 staining density, the optical intensity readings were corrected for nonspecific background, as measured from the corpus callosum for each animal. The fiber densities were expressed as the percent of intact side. The c-Fos and FosB positive cells were counted from 0.5 mm × 0.5 mm TIFF formatted images analyzed using the ImageJ software (Version 1.42i, NIH). After background subtraction, the numbers of cells specifically labeled with c-Fos and FosB were counted using the particle analysis tool. The density of immunopositive c-Fos and FosB profiles was expressed as number of cells/mm^2.

Confocal Microscopy. The triple immunohistochemical staining was visualized on a Nikon Eclipse 90i microscope equipped with a D-eclipse C1 confocal camera (Nikon). The high power confocal images were captured using a 60× Plan-Apo objective (Numerical aperture = 1.4) on a single plane using sequential acquisition. The low power images were taken using a 4× Plan-Fluor objective (numerical aperture = 0.13) as z-stacks of eight focal planes penetrating 6–8 μm from the surface of the section in sequential acquisition mode. Confocal images were captured and pseudo-colored using EZ-C1 software (gold version 3.9). The z-stack images were then processed for maximal intensity projection on an NIS-Elements AR software (version 3.10).

Stereological Analysis. The TH-positive and VMAT2-positive cell numbers in the SN were estimated using an unbiased stereological quantification method by using the optical fractionator principle (8, 9). All quantifications were done after blinding the identity of the sections by a coding system. Upon completion of the quantification of batches, samples were moved to a database for further analysis using appropriate statistical and graphical tools. The borders for the region of interest was defined by using a 4× objective, whereas the actual counting was performed using a 60× Plan-Apo oil objective (Numerical aperture = 1.4) on a Nikon 80i microscope equipped with an X-Y motorized stage, a *z* axis motor and a high-precision linear encoder (Heidenhein). All three axes and the input from the digital camera were controlled by a PC computer running the NewCast Module in VIS software (Visiopharm A/S), which carries out the procedure with a random start and systematic sampling routine. The sampling interval in the *x-y* axis was adjusted so that at least 100 cells were counted for each SN. Coefficient of error attributable to the sampling was calculated according to Gundersen and Jensen (10) and values ≤0.10 were accepted.

Statistical Analysis. Statistical significance for the group comparisons for stereological cell counts, fiber density measurements and the HPLC data were analyzed by using two-way factorial ANOVA, followed by post hoc comparisons using Tukey HSD test. One-way ANOVA test was performed to compare results from microdialysis measurements and the quantification of immediate-early gene markers, followed by Tukey HSD post hoc test. The above-mentioned data were represented as mean ± SE of mean. As AIM scores are not parametric data, they are presented as median ± 75% confidence interval. The final L-DOPA challenge scores were represented as a box-plot chart where the whiskers represent 95% percentiles of the median. The comparisons of the dyskinesia scores were performed using Friedman test followed by individual comparisons using Kolmogorov-Smirnov test and corrected for false discovery rate. Statistical significance was set at $P < 0.05$. All statistical analysis was performed using SPSS statistical software (Version 17).

1. Ulusoy A, Sahin G, Björklund T, Aebischer P, Kirik D (2009) Dose optimization for long-term rAAV-mediated RNA interference in the nigrostriatal projection neurons. *Mol Ther* 17:1574–1584.
2. Zolotukhin S, et al. (1999) Recombinant adeno-associated virus purification using novel methods improves infectious titer and yield. *Gene Ther* 6:973–985.
3. Grimm D (2002) Production methods for gene transfer vectors based on adeno-associated virus serotypes. *Methods* 28:146–157.
4. Paxinos G, Watson C (2007) *The Rat Brain in Stereotaxic Coordinates* (Academic Press, London), 2nd Ed.
5. Kirik D, Rosenblad C, Björklund A (1998) Characterization of behavioral and neurodegenerative changes following partial lesions of the nigrostriatal dopamine system induced by intrastriatal 6-hydroxydopamine in the rat. *Exp Neurol* 152:259–277.
6. Lundblad M, et al. (2002) Pharmacological validation of behavioural measures of akinesia and dyskinesia in a rat model of Parkinson's disease. *Eur J Neurosci* 15: 120–132.
7. Winkler C, Kirik D, Björklund A, Cenci MA (2002) L-DOPA-induced dyskinesia in the intrastriatal 6-hydroxydopamine model of parkinson's disease: Relation to motor and cellular parameters of nigrostriatal function. *Neurobiol Dis* 10:165–186.
8. West MJ (1999) Stereological methods for estimating the total number of neurons and synapses: Issues of precision and bias. *Trends Neurosci* 22:51–61.
9. Schmitz C, Hof PR (2005) Design-based stereology in neuroscience. *Neuroscience* 130: 813–831.
10. Gundersen HJ, Jensen EB (1987) The efficiency of systematic sampling in stereology and its prediction. *J Microsc* 147:229–263.

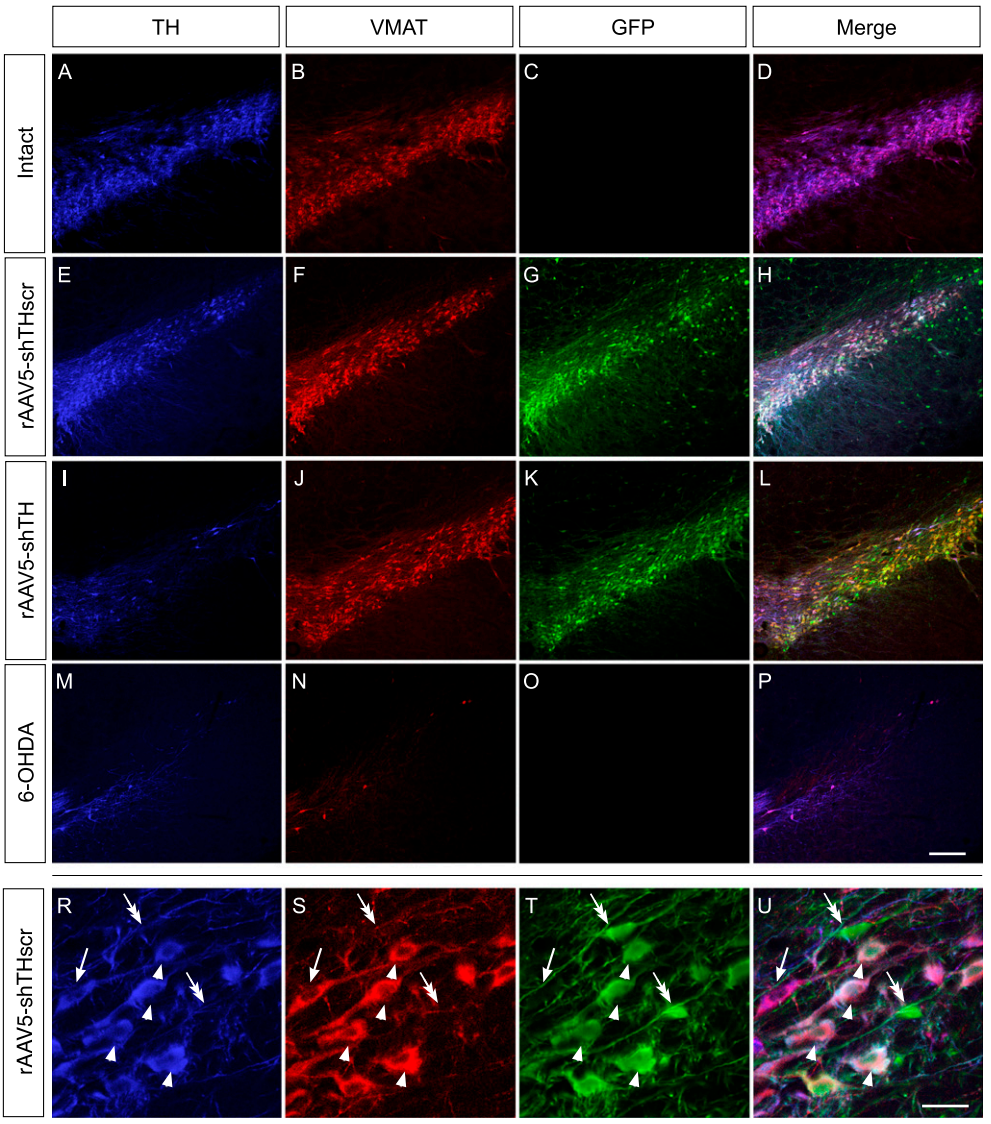

Fig. S1. Transgene expression and transduction efficacy following rAA5 mediated shRNA expression in the rat nigra. As the vector constructs express not only the shRNA but also the GFP marker protein, multilabeling using fluorescent immunohisochemistry allowed us to assess the transduction efficiency in the target cell population in the ventral midbrain. Confocal microscopical images are obtained from the substantia nigra after triple staining for TH pseudocolored in *blue* (*Left*), VMAT2 pseudocolored as *red* (*Center Left*), the GFP shown in *green* (*Center Right*) and the merged panels (*Right*) on the intact side (*A–D*), rAAV5-shTHscr (*E–H*), rAAV5-shTH (*I–L*) vector injected sides or in 6-OHDA lesioned rats (*M–P*). High power images obtained from rAAV5-shTHscr injected midbrain illustrates the colocalization of the three markers showing high efficiency of targeting the transgene to DA neurons (*R–U*). Injection of rAAV5-shTH (*I–L*) and rAAV5-shTHscr (*E–H*) leads to a robust GFP expression in the TH and VMAT2-positive neurons in the SN with high transduction efficiency. shTH expression led to specific down-regulation of the TH protein (*I*), whereas in the shTHscr group all three proteins are readily detectable giving the white color in the merged panels (*H*, *U*). Arrowheads show some of the triple labeled cells expressing the GFP marker gene, TH and VMAT2, arrow shows a nontransduced DAergic neuron expressing TH and VMAT2 but not GFP and two double arrows show GFP-positive transduced cells that are negative for both DAergic markers. (Scale bar, 200 μm in *P* for *A–P* and 30μm in U for *R–U*.)

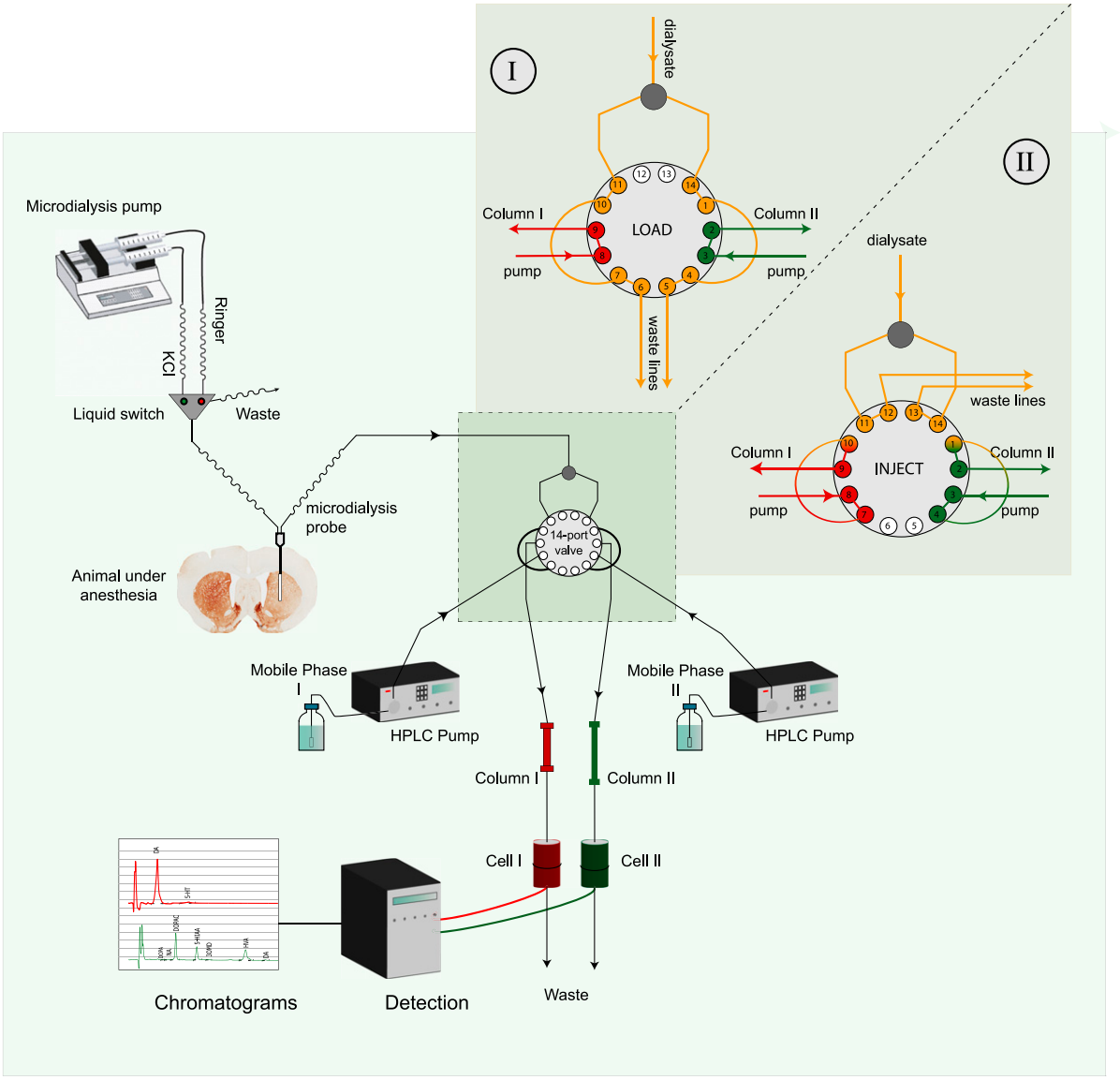

Fig. S2. Illustration of the ALEXYS Online Monoamine Analzyer. The microdialysis pump directs the ringer solution and the KCl solution to a liquid switch where depending on the experimental phase, either one of the solution is manually selected to flow into the microdialysis probe. We have, in this study, stereotaxically inserted the probe into the striatum of rats to measure extracellular levels of monoamines and their metabolites. The output dialysate collected from the striatum flows into 14-port injector valve and splits into two equal portions, eventually to be directed into two different columns for separate electrochemical detection. This separation allows acquiring increased time resolution and decreased sample volume. Two different valve positions define the flow paths of the mobile phases and the dialysate sample. When the valve is in load position (detailed in *I*) the dialysate is parallel loaded into two loops with 5-μL volume. The valve changes to the inject position at predefined time intervals. The residual volume exceeding 5 μL is disposed through waste lines. In the inject position (detailed in *II*) 5 μL dialysate sample is transferred from the loop to the columns. In this context we have used two different columns allowing us to detect NA, DA, and 5-HT in column 1 and NA, DOPA, DOPAC, 5-HIAA, 3-OMD, HVA and DA in column 2, simultaneously. Columns are connected to separate electrochemical cells and the signal is then detected and monitored as chromatograms.

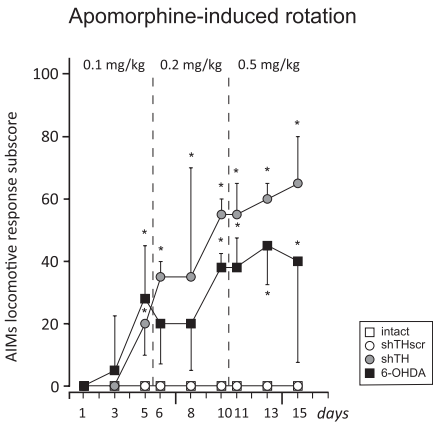

Fig. S3. Induction of locomotive dyskinesia observed as rotational behavior after daily apomorphine treatment using a dose-escalation regimen. Animals were scored three times at each dose level for development of AIMs by using a dedicated rating scale. Three subtypes of AIMs (forelimb, orolingual, and axial) are reported as integrated AIMs scores in Fig. 4. Locomotive behaviors were distinguished as circular movements contralateral to the lesioned side and were rated from 0 (absent) to 4 (continuous rotation, not interrupted by repeated strong sensory stimuli) every 10 min after each dose of apomorphine injections. In the shTH group there was slow onset but a continuous sensitization in the frequency of rotational response with escalating apomorphine doses. In the 6-OHDA lesion group, the overall response was not different from the shTH group, although the magnitude of the response was blunted with higher doses most likely due to severe axial dyskinesia seen in this group. Data are shown as median values in all groups. Error bars show 75% percentiles. Individual comparisons were performed by Kolmogorov-Smirnov test and *P* values were compensated for false discovery rates. *different from intact and shTHscr controls.

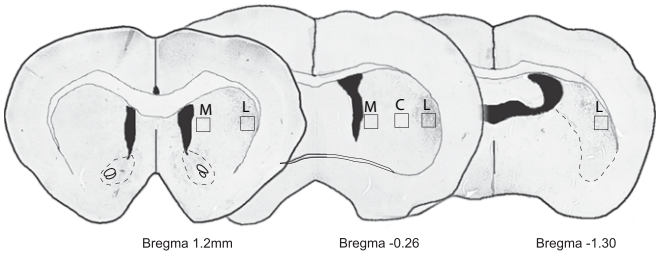

Fig. S4. Illustration of regions of interest used for quantification of the numbers of c-Fos and FosB-positive cells. The analysis was carried out on three coronal sections in the striatum at levels +1.2 mm, −0.26 mm, and −1.3 mm from bregma. Digital images were taken from the lateral striatum on all three levels, central striatum at the second level, and in the medial striatum at the first two levels as shown in the delineated squares.

Table S1. DA and DA metabolite levels in the dorsal striatum

	DA		DOPAC		HVA		(DOPAC + HVA)/DA	
	Baseline	L-DOPA	Baseline	L-DOPA	Baseline	L-DOPA	Baseline	L-DOPA
Right (injected)								
intact	55,533 ± 4,130	62,905 ± 8,761	4,596 ± 324	9,699 ± 1,043	2,773 ± 245	18,201 ± 3,073	0.135 ± 0.019	0.447 ± 0.032
shTHscr	46,774 ± 2,053	43,496 ± 4,614	3,182 ± 230	6,375 ± 262	2,126 ± 107	13,566 ± 1,022	0.114 ± 0.007	0.470 ± 0.052
shTH	31,012 ± 2,865*	56,587 ± 10,413	2,109 ± 162*	8,389 ± 1,664	1,242 ± 91*	12,535 ± 2,330	0.109 ± 0.005	0.372 ± 0.029
6-OHDA	1,099 ± 662*	9,218 ± 3,031	202 ± 99*	3,976 ± 1,080*	162 ± 62*	9,086 ± 3,157	0.588 ± 0.135*	1.558 ± 0.317*
Left (uninjected)								
intact	59,449 ± 4,502	50,571 ± 7,359	5,098 ± 168	6,666 ± 1,059	3,021 ± 231	14,577 ± 1,529	0.138 ± 0.011	0.437 ± 0.042
shTHscr	64,422 ± 3,444	50,589 ± 4,862	5,052 ± 396	7,211 ± 359	3,127 ± 143	14,930 ± 1,500	0.128 ± 0.009	0.444 ± 0.036
shTH	64,332 ± 3,684	59,117 ± 4,741	5,545 ± 304	10,316 ± 1,504	3,594 ± 201	16,004 ± 1,483	0.144 ± 0.009	0.445 ± 0.036
6-OHDA	50,649 ± 2,965	54,222 ± 5,678	4,914 ± 453	9,363 ± 2,530	2,887 ± 51	19,673 ± 5,364	0.151 ± 0.005	0.519 ± 0.084

Table contains two panels showing the right (injected) side and left (uninjected) side. Levels of DA, DOPAC, HVA and DA turnover rate in the dorsal striatum are illustrated under baseline conditions as well as in a group of animals that received a single dose of 12 mg/kg L-DOPA (plus 10 mg/kg benserazide) and killed 150 min after injection. The levels of DA, DOPAC, HVA, 5-HT and 5-HIAA are represented as fmol/mg tissue. Statistical group comparisons were performed using one-way ANOVA, if significant followed by Tukey HSD post hoc analysis. 5-HIAA, 5-hydroxyindoleacetic acid, 5-HT, serotonin; 6-OHDA, 6-hydroxydopamine; DA, dopamine; DOPAC, 3,4-dihydroxyphenylacetic acid; HVA homovanilic acid; scr, scrambled; shRNA, short hairpin RNA; shTH, short-hairpin RNAs targeting the rat TH mRNA.
*Different from intact controls.

Table S2. DA and DA metabolite levels in the ventral striatum including nucleus accumbens

	DA		DOPAC		HVA		(DOPAC + HVA)/DA	
	Baseline	L-DOPA	Baseline	L-DOPA	Baseline	L-DOPA	Baseline	L-DOPA
Right (injected)								
intact	40,261 ± 6,159	39,970 ± 7,648	4,449 ± 588	7,631 ± 1,696	2,427 ± 419	12,045 ± 1,776	0.181 ± 0.010	0.500 ± 0.021
shTHscr	35,503 ± 1,623	25,247 ± 7,242	3,403 ± 242	5,607 ± 2,423	1,837 ± 61	9,350 ± 3,507	0.149 ± 0.011	0.535 ± 0.123
shTH	29,239 ± 3,395	40,741 ± 3,213	2,745 ± 205	9,027 ± 1,223	1,412 ± 95*	11,400 ± 1,202	0.146 ± 0.007	0.502 ± 0.062
6-OHDA	5,934 ± 2,826	25,806 ± 2,817	929 ± 432*	7,812 ± 1,299	488 ± 174*	11,399 ± 2,878	0.313 ± 0.047*	0.729 ± 0.079
Left (uninjected)								
intact	45,689 ± 3,509	42,185 ± 1,797	5,241 ± 408	8,221 ± 600	2,429 ± 80	13,600 ± 1,441	0.177 ± 0.018	0.517 ± 0.048
shTHscr	39,317 ± 2,724	29,525 ± 1,448	4,392 ± 333	6,274 ± 794	1,905 ± 110	11,011 ± 3,258	0.163 ± 0.013	0.579 ± 0.091
shTH	35,374 ± 3,294	33,422 ± 3,706	4,134 ± 356	8,130 ± 1,373	2,083 ± 113	10,756 ± 1,881	0.179 ± 0.013	0.551 ± 0.049
6-OHDA	40,748 ± 2,902	40,130 ± 1,262	5,901 ± 434	10,322 ± 1,729	2,300 ± 148	17,856 ± 3,783	0.203 ± 0.008	0.695 ± 0.112

Table contains two panels showing the right (injected) side and left (uninjected) side. Levels of DA, DOPAC, HVA and DA turnover rate in the ventral striatum including nucleus accumbens are illustrated under baseline conditions as well as in a group of animals that received a single dose of 12 mg/kg L-DOPA (plus 10 mg/kg benserazide) and killed 150 min after injection. The levels of DA, DOPAC, HVA, 5-HT and 5-HIAA are represented as fmol/mg tissue. Statistical group comparisons were performed using one-way ANOVA, if significant followed by Tukey HSD post hoc analysis. 5-HIAA, 5-hydroxyindoleacetic acid, 5-HT, serotonin; 6-OHDA, 6-hydroxydopamine; DA, dopamine; DOPAC, 3,4-dihydroxyphenylacetic acid; HVA homovanilic acid; scr, scrambled; shRNA, short hairpin. RNA; shTH, short-hairpin RNAs targeting the rat TH mRNA.
*Different from intact controls.

Table S3. 5HT and 5HIAA levels in the dorsal striatum

	5HT		5HIAA		5HIAA/5HT	
	Baseline	L-DOPA	Baseline	L-DOPA	Baseline	L-DOPA
Right (injected)						
intact	1,010 ± 57	1,080 ± 314	1,078 ± 28	2,264 ± 232	1.097 ± 0.064	2.411 ± 0.404
shTHscr	791 ± 66	1,121 ± 300	914 ± 81	2,240 ± 271	1.160 ± 0.053	2.326 ± 0.303
shTH	970 ± 109	1,059 ± 246	1,013 ± 113	1,870 ± 180	1.049 ± 0.034	2.088 ± 0.235
6-OHDA	752 ± 201	1,229 ± 138	811 ± 133	2,958 ± 206	1.198 ± 0.125	2.432 ± 0.110
Left (uninjected)						
intact	1,359 ± 95	1,102 ± 181	1,503 ± 80	2,063 ± 235	1.122 ± 0.030	2.233 ± 0.194
shTHscr	1,476 ± 136	953 ± 100	1,694 ± 149	2,140 ± 306	1.155 ± 0.067	2.559 ± 0.166
shTH	1,384 ± 144	880 ± 90	1,618 ± 171	1,927 ± 156	1.174 ± 0.067	2.347 ± 0.205
6-OHDA	1,408 ± 117	1,237 ± 89	1,635 ± 95	2,606 ± 113	1.177 ± 0.038	2.117 ± 0.074

Table contains two panels showing the right (injected) side and left (uninjected) side. Levels of 5-HT, 5-HIAA and serotonin turnover rate in the dorsal striatum under baseline conditions and after L-DOPA injection were also measured to assess the specificity of the changes in the DAergic system. The levels of DA, DOPAC, HVA, 5-HT and 5-HIAA are represented as fmol/mg tissue. Statistical group comparisons were performed using one-way ANOVA, if significant followed by Tukey HSD post hoc analysis. 5-HIAA, 5-hydroxyindoleacetic acid, 5-HT, serotonin; 6-OHDA, 6-hydroxydopamine; DA, dopamine; DOPAC, 3,4-dihydroxyphenylacetic acid; HVA homovanilic acid; scr, scrambled; shRNA, short hairpin RNA; shTH, short-hairpin RNAs targeting the rat TH mRNA.
*Different from intact controls.

Table S4. 5HT and 5HIAA levels in the ventral striatum including nucleus accumbens

	5HT		5HIAA		5HIAA/5HT	
	Baseline	L-DOPA	Baseline	L-DOPA	Baseline	L-DOPA
Right (injected)						
intact	1,915 ± 343	2,264 ± 360	1,283 ± 210	2,666 ± 414	0.712 ± 0.033	1.346 ± 0.051
shTHscr	2,236 ± 126	1,780 ± 61	1,377 ± 97	2,168 ± 833	0.621 ± 0.043	1.684 ± 0.012
shTH	2,600 ± 335	2,361 ± 47	1,522 ± 185	3,672 ± 564	0.589 ± 0.019	1.481 ± 0.432
6-OHDA	2,615 ± 428	2,426 ± 160	1,464 ± 151	3,585 ± 133	0.587 ± 0.060	1.484 ± 0.042
Left (uninjected)						
intact	2,634 ± 242	3,116 ± 387	1,849 ± 89	2,945 ± 209	0.747 ± 0.034	1.074 ± 0.120
shTHscr	2,661 ± 372	2,022 ± 571	1,652 ± 228	2,380 ± 693	0.628 ± 0.034	1.517 ± 0.140
shTH	3,148 ± 223	1,722 ± 381	2,023 ± 260	2,366 ± 280	0.635 ± 0.052	1.276 ± 0.151
6-OHDA	2,713 ± 355	2,801 ± 260	1,962 ± 105	4,002 ± 265	0.753 ± 0.059	1.437 ± 0.065

Table contains two panels showing the right (injected) side and left (uninjected) side. Levels of 5-HT, 5-HIAA and serotonin turnover rate in the ventral striatum and nucleus accumbens under baseline conditions and after L-DOPA injection were also measured to assess the specificity of the changes in the DAergic system. The levels of DA, DOPAC, HVA, 5-HT and 5-HIAA are represented as fmol/mg tissue. Statistical group comparisons were performed using one-way ANOVA, if significant followed by Tukey HSD post hoc analysis. 5-HIAA, 5-hydroxyindoleacetic acid, 5-HT, serotonin; 6-OHDA, 6-hydroxydopamine; DA, dopamine; DOPAC, 3,4-dihydroxyphenylacetic acid; HVA homovanilic acid; scr, scrambled; shRNA, short hairpin RNA; shTH, short-hairpin RNAs targeting the rat TH mRNA.

*Different from intact controls.